Three-dimensional nanojunction device models for photovoltaics

Artit Wangperawong[1] and Stacey F. Bent[2,a)]
[1]*Department of Electrical Engineering, Stanford University, Stanford, California 94305, USA*
[2]*Department of Chemical Engineering, Stanford University, Stanford, California 94305, USA*

(Received 1 March 2011; accepted 6 May 2011; published online 8 June 2011)

A model is developed to describe the behavior of three-dimensionally nanostructured photovoltaic devices, distinguishing between isolated radial pn junctions and interdigitated pn junctions. We examine two specific interdigitated architectures, the point-contact nanojunction and the extended nanojunction, which are most relevant to experimental devices reported to date but have yet to be distinguished in the field. The model is also applied to polycrystalline CdTe devices with inverted grain boundaries. We demonstrate that for CdTe/CdS solar cells using low-quality materials, the efficiency of the extended nanojunction geometry is superior to other designs considered. © *2011 American Institute of Physics*. [doi:10.1063/1.3595411]

Predicated on the promise of enhanced charge collection,[1] extensive efforts have been made to fabricate efficient nanostructured photovoltaic devices. Despite good experimental progress,[2–7] fundamental analysis of carrier diffusion and collection in such geometries is limited. Previous three-dimensional (3D) analyses considered only isolated radial pn junctions pillars,[1,7,8] which do not accurately reflect works involving interdigitated, non-isolated pn junctions. In an interdigitated geometry, photogenerated carriers within a unit cell can diffuse to any one of the nearby junctions, not just the junction in the unit cell. As one of the primary purposes of nanostructuring is to reduce the charge collection distance, a complete analysis should include this effect. Here our modeling demonstrates that interdigitated junctions can offer superior performance over that of isolated radial junction and planar geometries.

Existing theoretical studies on the interdigitated geometry has not fully accounted for the 3D behavior of devices. For analyses in two-dimensions,[2,9] the geometrical effect of three-dimensions on depletion width, dark current, and space charge recombination are not properly treated. Studies that cylindrically integrate two-dimensional numerical simulations suffer the same limitations, as well as having unit cell boundary conditions that do not properly represent an interdigitated device.[7,8] Although full 3D analysis has not been practical numerically due to the computational resources required, here we take an analytical approach to best represent nanostructured photovoltaic geometries under experimental consideration today.

The two device architectures for interdigitated designs used in prior experiments are shown in Figs. 1 and 2.[2,3] We term them *the point-contact nanojunction* and *the extended nanojunction*. Previous studies do not distinguish between the two designs, but the difference in device performance is non-trivial. In both designs the absorber material is typically p-type, i.e., the base. It serves as the primary absorber material due to its greater minority carrier diffusion length in comparison to the heavily-doped n-type emitter. The emitter's main function is to aid carrier collection by producing a built-in field extending into the absorber. It is preferably a high-band gap material and occupies as small a volume as practicable to minimize parasitic absorption while maintaining the full built-in potential. Emitter contact for the extended device may occur on the entire top side, e.g., via a transparent conductor, whereas for the point-contact device it is made locally at each vertical junction. Together the base and emitter comprise a matrix of interdigitated nanojunctions that we model.

We begin with an effective medium approximation to model the effect of interdigitated junctions on the minority carrier diffusion in the base.[10] The minority carrier transport and collection properties in a cylindrical unit cell of radius a can be calculated by considering the charge collection probability φ. φ is defined as the fraction of photogenerated minority carriers at a point r which diffuse to a depletion edge, get collected, and contribute to photocurrent.[11] The value of φ embodies the response of the device to local low-level carrier generation. Furthermore, φ obeys its own diffusion equation according to the reciprocity theorem,[12]

$$\frac{1}{r}\frac{\partial}{\partial r}\left(r\frac{\partial \varphi_m}{\partial r}\right)+\frac{\partial^2 \varphi_m}{\partial z^2}-\frac{1}{L_m^2}\varphi_m=0 \quad m=1,2, \tag{1}$$

where φ_1 is the solution within the unit cell ($r \leq a$) and φ_2 is the solution outside ($r \geq a$). The minority carrier diffusion

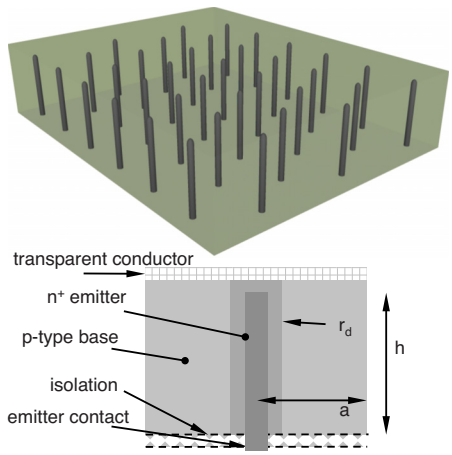

FIG. 1. (Color online) The point-contact nanojunction design and relevant components of each unit cell.

a)Author to whom correspondence should be addressed. Present address: Stanford University, 381 North South Axis, Stanford, California 94305, USA. Electronic mail: sbent@stanford.edu. Tel.: +1-650-723-0385. FAX: +1-650-723-9780.

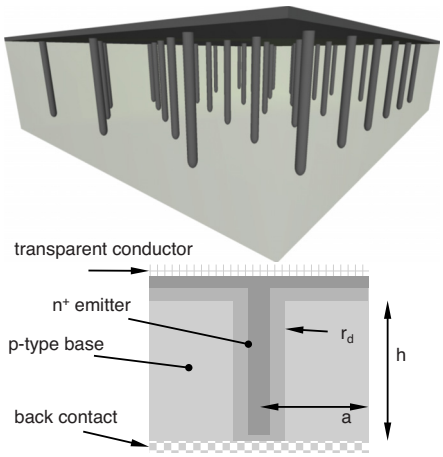

FIG. 2. (Color online) The extended nanojunction design and relevant components of each unit cell.

length L_1 in the cylindrical unit cell can be used to model the effective minority carrier diffusion length L_2 outside by self-consistent averaging. Once φ_1 is known, the reciprocal relationship between dark carrier distribution and photogenerated carrier collection enables us to calculate the photocurrent, ideal dark current, and depletion region recombination current. Hereon the latter two together normalized to the illumination area will be called J_{dark}. We then superimpose these contributions to obtain the overall J-V curves (Fig. 3). For more details, see Ref. 13.

While there are many parameters to explore in a photovoltaic device, we restrict ourselves to two extreme cases—high- and low-quality materials—and in our case, we consider CdTe/CdS devices. We assume that for high-quality CdTe, which is desirable for planar cells, the acceptor doping concentration N_a is relatively low and the minority carrier lifetime τ_n and mobility μ_n are both higher than the low-quality case (Table I).[2,8,14,15] This requires that the effect of defects between vertical junctions be represented by those variables.

There is evidence that $CdCl_2$ vapor treatment of polycrystalline CdTe induces inversion at grain boundaries (GBs) which aids photogenerated electron collection.[16] This effect would be negligible for the point-contact and extended nanojunction models due to the length scale difference between vertical junctions and GBs. Nevertheless, a different architecture involving vertically extended junctions at the GBs, here termed *inverted GBs*, can be described. Using the modeling approach presented above, we have included J-V curves (Fig. 3) of inverted GB devices with 4 μm diameter grains,[17] each grain interior having properties of Table I.

TABLE I. Properties used to model high- and low-quality CdTe.

Property	High	Low
Acceptor doping, N_a (cm^{-3})	2×10^{14}	1×10^{17}
Electron mobility, μ_n ($cm^2/V\ s$)	320	100
Electron lifetime, τ_n (ns)	1	1×10^{-2}
Diffusion length, L_n (μm)	0.910	0.050
Absorber thickness, h (μm)	3.0	1.0

Previous studies suggest that polycrystalline CdTe (Ref. 16) and CIGS (Refs. 18–20) devices outperform their corresponding single crystal ones because the inverted GB interior is higher quality than the large single crystal. Our results are corroborative in that the high-quality inverted GB device is shown to outperform the low-quality planar device. The point-contact and extended junction designs are nevertheless important to examine, as the fortuitous GB inversion and gettering observed in $CdCl_2$-treated CdTe does not occur in all materials. Moreover, our results show that the nanojunction architectures outperform the inverted GB device when low quality CdTe is used.

Consider first the high-quality devices in Fig. 3(a). While the extended junction design provides higher collection probability throughout the device than the other geometries, it also leads to higher J_{dark} as apparent in its lower open-circuit voltage V_{oc}. As for short-circuit current, the extended junction geometry does not make a significant difference because of high L_1 and the field-assisted carrier collection that already exists in the horizontal depletion region. In other words, the depletion width extending into a high-quality planar CdTe absorber over the biases of interest is already comparable to the average photon absorption depth.

On the other hand, V_{oc} for the point-contact geometry is greater than that of the extended case, an effect due to the reduced junction interfacial area giving rise to J_{dark}. Unfortunately, a virtual shunt caused by the field-dependent carrier collection reduces the fill-factor. This is expected since the photogeneration intensity exponentially decays with depth while the photogenerated carriers diffuse laterally to be collected. For these reasons, planar devices are superior for high-quality CdTe.

Considering next the low-quality devices in Fig. 3(b), we note that the depletion region is substantially reduced because of the heavier base doping. The average photon absorption depth is now greater than the depletion width of the planar device. The diffusion length is also now much shorter. The enhanced collection probabilities of the nanojunction geometries here play a pivotal role in terms of efficiency. In

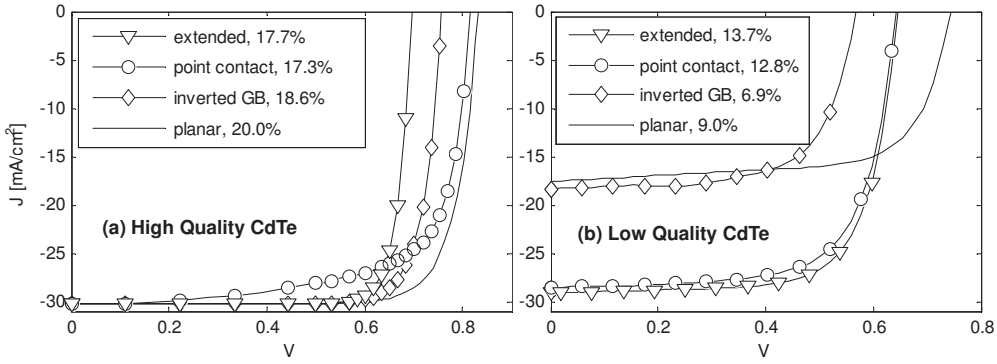

FIG. 3. Optimized performance of (a) high quality and (b) low quality CdTe/CdS solar cells of various device geometries under AM 1.5G illumination. All properties are equal aside for those specified in Table I. Inset: legend with efficiencies. For comparison, 3 μm-thick low-quality devices are 12.7%, 11.9%, 6.0%, and 9.0%, respectively.

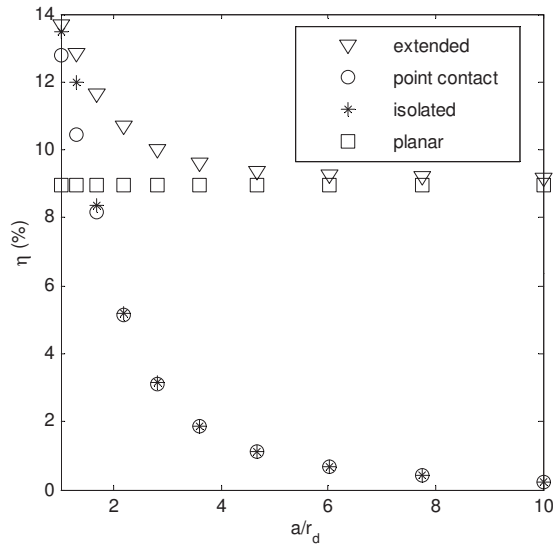

FIG. 4. Low-quality CdTe/CdS solar cell efficiencies for various device architectures as a function of spacing between vertical nanojunctions. The unit cell radius a is normalized to the equilibrium depletion radius r_d on the horizontal axis.

order to maintain high collection probabilities throughout the device, the vertical junctions need to be positioned closer to one another than the high-quality case above. This increase in junction interfacial area increases J_{dark}, an undesired consequence that can be mitigated by making the vertical junctions shorter. The absorber layer can then be as thin as possible to maintain adequate absorption. The nanojunction devices outperform the planar one given a 3 μm thick absorber but are even more advantageous with a reduction to 1 μm. In both cases the nanojunction devices have lower V_{oc} than the planar one but can produce more photocurrent.

Figure 4 plots low-quality CdTe/CdS solar cell efficiencies calculated for various device architectures as a function of the spacing between vertical nanojunctions. The ideal case of zero surface recombination and 100% packing factor is assumed for the isolated radial pn junction array devices. For all of the architectures, the optimal condition is when the nanojunctions are close enough for neighboring depletion edges in the vertical direction to meet, thereby maximizing the field-assisted carrier collection. It is necessary to space the vertical junctions as close as possible because the minority carrier diffusion length is only 50 nm (see Table I). The increase in J_{dark} due to the higher density of vertical junctions does not overshadow the efficiency gains. Compared to other nanojunction device studies that accounted for radial variation,[1] the efficiency advantage over the planar device does not rely on operating in full depletion nor assume a higher lifetime in the depletion region than that of the quasineutral region.

As the unit cell radius a increases to large values in comparison to the minority carrier diffusion length L_1, Fig. 4 shows that the performance of the extended junction device approaches that of the planar one. Before reaching this limit, the extended junction device always outperforms the planar one. On the other hand, the efficiencies of the point-contact and isolated radial pn junction pillars approach zero as a becomes large. This is to be expected, as there is almost no charge collection area in this limit. Therefore the extended junction device appears to be a more robust design for low-quality CdTe/CdS solar cells.

In conclusion, we demonstrate through our model that for CdTe/CdS solar cells the nanojunction devices are advantageous for low-quality absorbers with higher doping and lower minority carrier mobility and lifetime. The extended junction architecture consistently outperforms all other devices considered for various vertical junction densities. These results have important implications for proper design of high-performing solar cells made of inexpensive and low-quality materials, especially for previously examined and emerging solar cell materials without the option of inverted GBs or gettering. With increasing attention in highly nanostructured devices, such as extremely thin absorber cells,[21] the analytical approach presented will be useful for modeling various geometries and materials systems. Applications beyond photovoltaics include diffusion-based devices such as photoelectrochemical cells and photocatalytic devices.

Studies were carried out as part of the Center on Nanostructuring for Efficient Energy Conversion, an EFRC funded by the U.S. Department of Energy, Office of Basic Energy Sciences under Award No. DE-SC0001060. A.W. acknowledges financial support from the DOE, Office of Science Graduate Fellowship Program, made possible in part by the American Recovery and Reinvestment Act of 2009, administered by ORISE-ORAU under Contract No. DE-AC05-06OR23100, and support from National Science Foundation under Grant No. CBET 0930098.

[1] B. M. Kayes, H. A. Atwater, and N. S. Lewis, J. Appl. Phys. **97**, 114302 (2005).
[2] Z. Fan, H. Razavi, J. Do, A. Moriwaki, O. Ergen, Y.-L. Chueh, P. W. Leu, J. C. Ho, T. Takahashi, L. A. Reichertz, S. Neale, K. Yu, M. Wu, J. W. Ager, and A. Javey, Nature Mater. **8**, 648 (2009).
[3] K.-Q. Peng, X. Wang, L. Li, X.-L. Wu, and S.-T. Lee, J. Am. Chem. Soc. **132**, 6872 (2010).
[4] M. C. Putnam, S. W. Boettcher, M. D. Kelzenberg, D. B. Turner-Evans, J. M. Spurgeon, E. L. Warren, R. M. Briggs, N. S. Lewis, and H. A. Atwater, Energy Environ. Sci. **3**, 1037 (2010).
[5] E. C. Garnett and P. D. Yang, J. Am. Chem. Soc. **130**, 9224 (2008).
[6] B. Tian, X. Zheng, T. J. Kempa, Y. Fang, N. Yu, G. Yu, J. Huang, and C. M. Lieber, Nature (London) **449**, 885 (2007).
[7] M. D. Kelzenberg, M. C. Putnam, D. B. Turner-Evans, N. S. Lewis, and H. A. Atwater, Proceedings of the 34th IEEE on Photovoltaic Specialists Conference, Philadelphia, P.A., 2009.
[8] R. Kapadia, Z. Fan, and A. Javey, Appl. Phys. Lett. **96**, 103116 (2010).
[9] W. K. Metzger, J. Appl. Phys. **103**, 094515 (2008).
[10] C. Donolato, Semicond. Sci. Technol. **15**, 15 (2000).
[11] M. A. Green, *Solar Cells: Operating Principles, Technology, and System Applications* (Prentice-Hall, New Jersey, 1982).
[12] C. Donolato, Appl. Phys. Lett. **46**, 270 (1985).
[13] See supplementary material at http://dx.doi.org/10.1063/1.3595411 for modeling details.
[14] S. Adachi, *Properties of Group-IV, III-V and II-VI Semiconductors* (Wiley, West Sussex, England, 2005).
[15] M. Gleockler, A. L. Fahrenbruch, and J. R. Sites, Proceedings of World Conference Photovoltaic Energy Conversion, 2004 Vol. 3, p. 491.
[16] I. Visoly-Fisher, S. R. Cohen, K. Gartsman, A. Ruzin, and D. Cahen, Adv. Funct. Mater. **16**, 649 (2006).
[17] J. Britt and C. Ferekides, Appl. Phys. Lett. **62**, 2851 (1993).
[18] C. Persson and A. Zunger, Phys. Rev. Lett. **91**, 266401 (2003).
[19] D. Azulay, O. Millo, I. Balberg, H.-W. Schock, I. Visoly-Fisher, and D. Cahen, Sol. Energy Mater. Sol. Cells **91**, 85 (2007).
[20] M. J. Hetzer, Y. M. Strzhemechny, M. Gao, M. A. Contreras, A. Zunger, and L. J. Brillson, Appl. Phys. Lett. **86**, 162105 (2005).
[21] *Nanostructured and Photoelectrochemical Systems for Solar Photon Conversion*, edited by M. D. Archer and A. J. Nozik (Imperial College Press, London, 2008).